Estimating Perfluorocarbon Emission Factors for Industrial Rare Earth Metal Electrolysis

Abstract:

Rare earth (RE) metals have been widely applied in new materials, leading to their drastic production increase in the last three decades. In the production process featured by the molten-fluoride electrolysis technology, perfluorocarbon (PFC) emissions are significant and therefore deserve full accounting in greenhouse gas (GHG) emission inventories. Yet, in the '*2006 IPCC Guidelines for National Greenhouse Gas Inventories*', no method currently exists to account for PFC emissions from rare earth metal production. This research aims to determine emission factors for industrial rare earth metals production through on-site monitoring and lab analysis of PFC concentrations in the exhaust gases from rare earth metal electrolysis. Continuous FTIR measurements and time-integrated samples (analysed off-site by high-precision Medusa GC-MS) were conducted over 24-60 hour periods from three rare earth companies in China, covering production of multiple rare earth metals/alloys including Pr-Nd, La and Dy-Fe. The study confirmed that PFC emissions are generated during electrolysis, typically in the form of CF_4 (~90% wt of detected PFCs), C_2F_6 (~10%) and C_3F_8 (<1%); trace levels of c-C_4F_8 and C_4F_{10} were also detected. In general, PFC emission factors vary with rare earth metal produced and from one facility to another, ranging from 26.66 to 109.43 g/t-RE for CF_4 emissions, 0.26 to 10.95 g/t-RE for C_2F_6, and 0.03 to 0.27 g/t-RE for C_3F_8. Converted to 211.60 to 847.41 kg CO_2-e/t-RE for total PFCs, this emissions intensity for rare earths electrolysis is of lower (for most RE production) or similar (Dy-Fe production) level of magnitude to industrial aluminium electrolysis.

Keywords: PFC, greenhouse gas, emission factor, rare earth metal, electrolysis

1. Introduction

1.1. Rare Earth Metals Production & PFC Greenhouse Gas Emissions

'Rare earth metals' typically refer to a set of chemical elements in the periodic table, i.e. the fifteen lanthanides as well as scandium and yttrium. Rare earth (RE) metals have significant applications in new materials which are in wide demand in emerging and advanced industries such as permanent magnets and high-performance electronic devices. Therefore, in the last three decades, production of rare earth metals has soared dramatically. For instance, the global annual production of $Nd_2Fe_{14}B$ permanent magnets have increased from around 1 tonne in the 1980s to more than 50,000 tonnes in around 2000 (Liu, 2008).

Since the 1990s, rare earth electrolysis using the molten *fluoride*-salt system has become the dominant production technology for rare earth metals. This replaced the molten *chloride*-salt system that was prevalent prior to the 1990s but suffered from several limitations, including: low

current efficiency, generation of chlorine gas as an environmental pollutant, poor metal quality / purity and other reasons.

The fluoride-based molten salts electrolysis process used today for rare earths production shares many similarities to the process used by the primary aluminium industry. As with aluminium electrolysis, the fluoride electrolysis route for rare earths production has the potential to form perfluorocarbon (PFC) gases, including tetrafluoromethane (CF_4, PFC-14) and hexafluoroethane (C_2F_6, PFC-116), both of which are potent greenhouse gases; octafluoropropane (C_3F_8, PFC-218) is also occasionally reported in aluminium. According to the *Intergovernmental Panel for Climate Change* (IPCC)'s *Fifth Assessment Report* (2013), CF_4 has an extremely long atmospheric lifetime of 50,000 years and a global warming potential (GWP100) of 6,630 compared to CO_2 over 100 years, C_2F_6 has a lifetime of 10,000 years and a GWP100 of 11,100, and C_3F_8 has a lifetime of 2,600 years and a GWP100 of 8,900.

While global production of rare earth metals by molten electrolysis technology is still very low compared to global aluminium production (roughly 0.1% of aluminium in 2013, based on global output of rare-earth oxides versus metallurgical-grade aluminium oxide (US Geological Survey 2014; IAI 2014)), it is possible that the resulting volume of greenhouse gas emissions can be comparatively large. Taking neodymium (Nd) metal production by Nd oxide electrolysis for example, it has been estimated by Vogel et al. (2017a) that in a *worst-case scenario*, the off-gases from the process could contain as much as 7% CF_4 and 0.7% C_2F_6. When considering the extremely large GWPs of these PFC gases and global production of roughly 30,000 t/year Nd metal, the rare earths industry could produce as much as 20 million t CO_2-e/year (Vogel et al., 2017a).

If a significant volume of PFC generation from the rare earths industry was confirmed, this would go towards explaining the large discrepancy or 'gap' that has been found between (i) global atmospheric measurements of PFC emissions (a 'top-down' approach for accounting PFCs) and (ii) global 'bottom-up' accounting of PFC emissions from aluminium and semi-conductor industries. Both these industries are currently considered the only major anthropogenic sources of PFCs, with both employing methodologies from the IPCC to account for PFC emissions. Using atmospheric data, Kim *et al.* (2014) showed that as much as 50% of CF_4 and 48% of C_2F_6 emissions over the 2002–2010 period (5,200 t/year CF_4 and 300 t/year C_2F_6, equivalent to 42 million t CO_2-e/year) is being under-estimated or unaccounted for from global industrial sectors.

The potential for large volumes of PFC gas emissions (combined with extremely high GWPs) from the rare earth metal industry implies that it should not be overlooked in terms of mitigating global warming. Therefore, evaluation and calculation of the global warming contribution from the rare earth metal industry is urgently needed. However, in the *2006 IPCC Guidelines for National Greenhouse Gas Inventories* (henceforth abbreviated to 2006 IPCC Guidelines), no guideline exists for the rare earth metal industry. One factor might have been the low proportion of Chinese contributors to the 2006 IPCC Guidelines (only 3.6% of authors and review editors for the entire 2006 IPCC Guidelines and only 1.1% for Volume 3 of the 2006 IPCC Guidelines: 'Industrial Processes & Product Use' (IPPU), where metal industry emissions are described) despite the fact that about 90% of rare earth metals globally are produced in China. Another more likely reason is that the global metal production of rare earths prior to 2006 was too small to consider as a significant contributor to GHG emissions, as already discussed above.

A further critical factor is the fact that to date there is a lack of quality academic research to

support a robust guideline for rare earth metal industry, if such a guideline were to be proposed. By contrast, there are numerous academic works and industrial studies on PFC emissions from primary aluminium production (Tabereaux, 1994; Rhoderick et al., 2001; Chase et al., 2005; Zhao et al., 2008; Wong et al., 2015). These have built up a robust foundation for the description of a detailed method for estimating PFC emissions from aluminium production in the 2006 IPCC Guidelines.

As a response to the above, recently a few studies on PFC emissions from the rare earth metals industry have been published. An example is the research conducted by Vogel et al. (2017a) who studied the electrochemistry of the neodymium oxide electrolytic system and the resulting anodic gas emissions. As the goal was to reduce PFC emissions, the paper focused on the interaction mechanism between CO/CO_2 and CF_4 emission concentrations and voltage across the electrochemical cell. With this groundwork, Vogel and Friedrich (2017b) continued the research and concluded that poor control of oxide concentrations of the electrolyte can cause higher PFC emissions. Therefore, a process control strategy similar to that in aluminium electrolysis was proposed to reduce PFCs, with continuous and precise oxide feeding being essential elements.

Vogel and his colleagues' research was conducted under laboratory conditions but mimicked industrial production. Given the variation of production engineering and gas scrubbing, this approach is effective in exploring the fundamental mechanisms of PFC emission but cannot be applied to estimating actual PFC emissions from the rare earth metal production industry. Therefore, Zhang et al. (2018) conducted research which measured continuous PFC emissions in an actual rare earth metal production facility. Zhang's work only focused on the PFC emission from production of Nd metal and Dy-Fe alloy at one rare earth production company. However, there are currently more than ten types of rare earth metals and alloys being produced by electrolysis every year. These include (in order of production output, from greatest to smallest): Pr-Nd, Nd, La, Dy-Fe, Ga-Fe, Ho-Fe, Pr, Ce, La-Ce and Y-Mg (ranking based on production data from major producers, covering 95% of the market). Furthermore, Zhang's data is limited in that it focused only on CF_4 emissions and did not measure other important PFC gases such as C_2F_6 and C_3F_8. Uncertainty analyses were also not provided from the study. Since the time of Zhang's measurements in 2014, there have also been significant improvements made in rare earth electrolysis technologies and in the operations of the process, which are expected to help reduce PFC emissions. Recently, for cleaner production, gas-collection hoods for each electrolytic cell have been applied in some newly established production shops. There was no estimation of gas collection efficiencies of the hooding systems (i.e. emission factors did not take into account any fugitive emissions) in Zhang's (2018) study, which is a further significant uncertainty in this previous work.

1.2. Aims of this Work

In light of the limitations of prior studies and the new developments in rare earth metal production, this paper goes further to measure PFC emissions from the production of Pr-Nd alloy, Dy-Fe alloy and La metal from different electrolytic cell sizes and gas exhaust systems. It aims to provide greater coverage of PFC emissions in the rare earth metal industry so that PFC emission factors for different rare earth metals produced with different technologies can be proposed. The measurement of the PFC emissions was conducted in three typical rare earth companies in

Ganzhou, Jiangxi province. These three companies consist of diversified technologies including old and new production shop settings, small and large electrolytic cells, and low and high cell current technologies.

1.3. The Fluoride Electrolysis Process for Rare Earth Metal Production

The dominant technology worldwide for primary production of RE metals and alloys is using molten fluoride-salt electrolytic reduction, similar to primary aluminum's Hall-Héroult process. The raw materials for rare earths metal production are in the form of rare earth oxides (REO). In general, REOs are dissolved and electrolytically reduced in a molten salt of rare earth fluorides (REF_s) and lithium fluoride (LiF), with graphite anodes and inert or consumable cathodes. The temperature in the reaction cell is high (~1000-1100 °C) and can vary depending on technology or metal produced, and be periodically interrupted or disturbed by anode replacements, cathode removal/replacement and removal of liquid RE metal/alloy.

Industrial fluoride-based rare earth smelters can be arbitrarily categorised into three classes by electrical current (and therefore the size of electrolysis cells), namely: low amperage (LA) technology, high amperage (HA) technology and high amperage with automatic control (HAA) technology. Low amperage technology (LA) are those with electrical current lower than 10 kA and typically employ small round-shaped cells, with only single (or several) vertical anodes and cathodes, and with very low levels of automation. For high amperage technology (HA and HAA), the current is higher than 10 kA. Typically, these use round or rectangular shaped cells, equipped with multiple vertical anodes and/or cathodes (Wen et al., 2012; Vogel & Friedrich, 2015). Some high amperage technologies may be equipped with 'Automatic Process Control' features (HAA), being able to automate rare earth oxide feeding so as to ensure continuous metal production and detection of anode effects that generate PFC.

PFC emissions are mainly in the form of CF_4 and C_2F_6 and are often associated with 'anode effects' (AEs), resulting in passivation of graphite anodes (loss of electrical current-carrying capacity) and high cell voltage. These PFC emissions may be produced in the following manner (taking Nd metal electrolysis as an example) (equations 1-4):

$$4NdF_3 + 3C \rightarrow 4Nd + 3CF_4 \quad \text{(Eq. 1)}$$

$$4LiF + C \rightarrow 4Li + CF_4 \quad \text{(Eq. 2)}$$

$$2NdF_3 + 2C \rightarrow 2Nd + C_2F_6 \quad \text{(Eq. 3)}$$

$$6LiF + 2C \rightarrow 6Li + C_2F_6 \quad \text{(Eq. 4)}$$

In addition to being directly formed by electrolysis (equations 1-4), PFCs can also be generated by first forming COF_2 or COF electrochemically at lower electrode potentials (equations 5-6), which are unstable and will spontaneously react with C to form CF_4 and CO (equations 7-8) as follows (Vogel 2017a, Kjos 2018):

$$Nd_2O_3 + 2NdF_3 + 3C \rightarrow 4Nd + 3COF_2 \quad \text{(Eq. 5)}$$

$$Nd_2O_3 + NdF_3 + 3C \rightarrow 3Nd + 3COF \quad \text{(Eq. 6)}$$

$$2COF_2 + C \rightarrow CF_4 + 2CO \quad \text{(Eq. 7)}$$

$$4COF + C \rightarrow CF_4 + 4CO \quad \text{(Eq. 8)}$$

2. Methodology

Two simultaneous methods were used for sampling PFC emissions: (i) continuous onsite monitoring with an FTIR and (ii) time-integrated sampling (collection of emissions into gas canisters) with offsite lab analysis. In this study we focused on estimating emission factors for CF_4, C_2F_6 and C_3F_8.

The most commonly applied equipment for monitoring PFC emissions is the *Fourier Transform Infrared* (FTIR) spectrometer. In theory, it is capable of capturing the emission data of all PFCs continuously in real-time. However, in RE metal production, in addition to emissions of major PFC gases (CF_4), there are minor PFCs including C_2F_6 and C_3F_8 which can be more difficult to detect with the FTIR. It must be noted that when measuring these emissions with the FTIR, gases will only be detected when emission concentrations exceed certain detection limits, an issue related to the reference spectrum used in the FTIR database. Therefore during gas measurements, it is crucial to record information relating to the configuration of the production system and ensure that the on-site gas monitoring point has sufficiently high emission concentrations. In this study, CF_4 emissions were primarily estimated using FTIR measurements, whereas C_2F_6 and C_3F_8 emissions were estimated using the time-integrated sampling and lab analysis technique.

As emissions from a single cell can differ from other cells due to variations in structure, operating conditions and production stage, it is better to monitor emissions from *a group of cells*, e.g. 12 cells or more, even up to one 'potroom' or 'potline' of cells (a chain of cells connected in series to the same electrical circuit and same exhaust gas system) so as to reduce inherent measurement error. However, the number of cells covered must be balanced by maintaining sufficiently high concentrations of CF_4, C_2F_6 and C_3F_8 that can still be accurately measured with the FTIR and time-integrated sampling. An optimum location can be in a common gas exhaust duct from a group of cells or from the gas stack before/after gas treatment for the entire potline.

Another issue that must be considered is the *gas collection efficiency*. During the monitoring process, the percentage of gases that is fully captured by the gas collection systems against all gases generated by the cells must be estimated. If gas collection efficiency is lower than 90% (i.e. more than 10% fugitive or uncontrolled emissions is not collected by the gas suction system), then there should be extra measurements of fugitive emissions at the exit point of the potroom/production shop where electrolysis cells are located, e.g. if there is a natural flow of air to the roof (Fraser et al., 2013). However, since the three rare earth companies monitored did not have any readily identifiable / accessible roof vents, gas collection efficiency was estimated at each company by releasing known quantities of SF_6 gas at the cell and using this as a tracer.

The amount of gas emissions in RE metal production can change over time. This may result from a variety of major process events on the cells, such as anode/cathode changes, metal removal, voltage/current change, RE oxide additions and the triggered 'anode effect' events. Therefore, to capture a representative period of operations/events, continuous measurements should ideally be conducted over a minimum of 24 hours (generally, the longer the time frame the better). During monitoring, all major process events were recorded so that any features in the gas concentrations can be correlated with these events – note that these features are not the focus of this paper and therefore are not elaborated further in this work. Furthermore, production data (metal and quantity produced) and technology factors (line current and cell size, which can fundamentally change the

emission outcomes) were also recorded.

For this research, three companies located in Ganzhou, Jiangxi province of China were selected as the representative cases: *Qiandong Rare Earths Group Co. Ltd* (Qiandong in abbreviation), *National Engineering Research Center for Ionic Rare Earth* (Ionic Rare Earth Center in abbreviation) and *Jiangxi South Rare Earth High Tech. Co. Ltd* (Jiangxi South in abbreviation). Qiandong specialises in three widely used RE metals including Pr-Nd alloy, La and Dy-Fe alloy. In contrast, Ionic Rare Earth Center attaches more importance on research, especially on new technologies for RE metals processing from ionic rare earths. Thus, measurement data from the Ionic Rare Earth Center can provide additional new information to the PFC emission spectrum. Jiangxi South was also included in the study as it employs some of the larger high-amperage (>10 kA) cell technologies.

In 2016, approximately half of China's RE metals are produced by companies/institutions in Ganzhou, and Qiandong accounts for more than 1/3 of the total production in Ganzhou. In light of the above, the three companies participating in this study can be a valid representation of PFC emissions in the RE metal production industries in China, or even in the world.

2.1. Continuous On-Site FTIR Monitoring

For on-site monitoring of the CF_4 emission, an FTIR spectroscopy instrument (*MKS MultiGas™ 2030 or MG2030*, which is competent in capture of CF_4 emissions) was employed. Where possible, we measured emissions from a series/group of pots so as to ensure data was representative and to minimise the risk of major inaccuracies that are more likely to occur in measuring single pots (Table 1). Figure 1 shows the schematic diagram of the intended sampling set up and process.

Table 1: Intended sampling arrangement for monitoring PFC emissions at the three RE companies

Company	Qiandong			Ionic Rare Earth Center	Jiangxi South
Potline (metal produced)	*Pr-Nd*	*Dy-Fe*	*La*	*Pr-Nd*	*Pr-Nd*
No. of cells/pots	15	1	6	6	2
Line current (kA)	5	5	5	6	11
Time frame (hours)	60	24	36	36	24
Monitoring equipment	*MKS MG2030* FTIR for continuous onsite gas analysis, with gases simultaneously collected in sampling canisters for offsite lab analysis				

As explained previously, in addition to CF_4 there are minor PFC gas emissions including C_2F_6 and C_3F_8 which cannot be easily detected by *MKS MG2030.* However, it is still important to estimate emission factors for these two critical PFC gases. To circumvent this issue, we also collected 'time-integrated' gas emission samples (simultaneously with FTIR measurements over the same sampling durations) and stored them in canisters for subsequent offsite lab analysis (Figure 1); offline analyses provided considerably lower detection limits for other C-F gases.

Through this approach, we estimate ratios of emission volumes for all other PFC components compared to CF_4, whereby emission factors for C_2F_6 and C_3F_8 can be calculated once CF_4 emission factors are known/confirmed – details are explained in section 2.4.

In this research, the emission factor of CF_4 (EF_{CF4}) is calculated directly by the equation below:

$$EF_{CF4} = \frac{[CF_4] \times t \times F \times 0.088}{22.4 \times 10^6 \times Ecol \times Q} \qquad \text{(Eq. 9)}$$

Where *[CF_4]* is volume concentration (ppmv), using data from the FTIR; *t* is total sampling time (*h*); *F* is the average gas flow rate at the sampling point *(Nm^3/h)*; *Ecol* is gas collection efficiency and *Q* is rare earth metal produced (tonnes) over the sampling time.

It was foreseeable during initial inspections that emissions from electrolysis cells could not be completely gathered and sent by gas collection systems to the exhaust gas stack, where sampling and measurements would be set up (Figure 1). Thus, a SF_6 tracer gas was employed to estimate the gas collection efficiency at each company. Once this is known, the volumes of all gas emissions can be calculated and accurate and reliable emission factors can then be estimated.

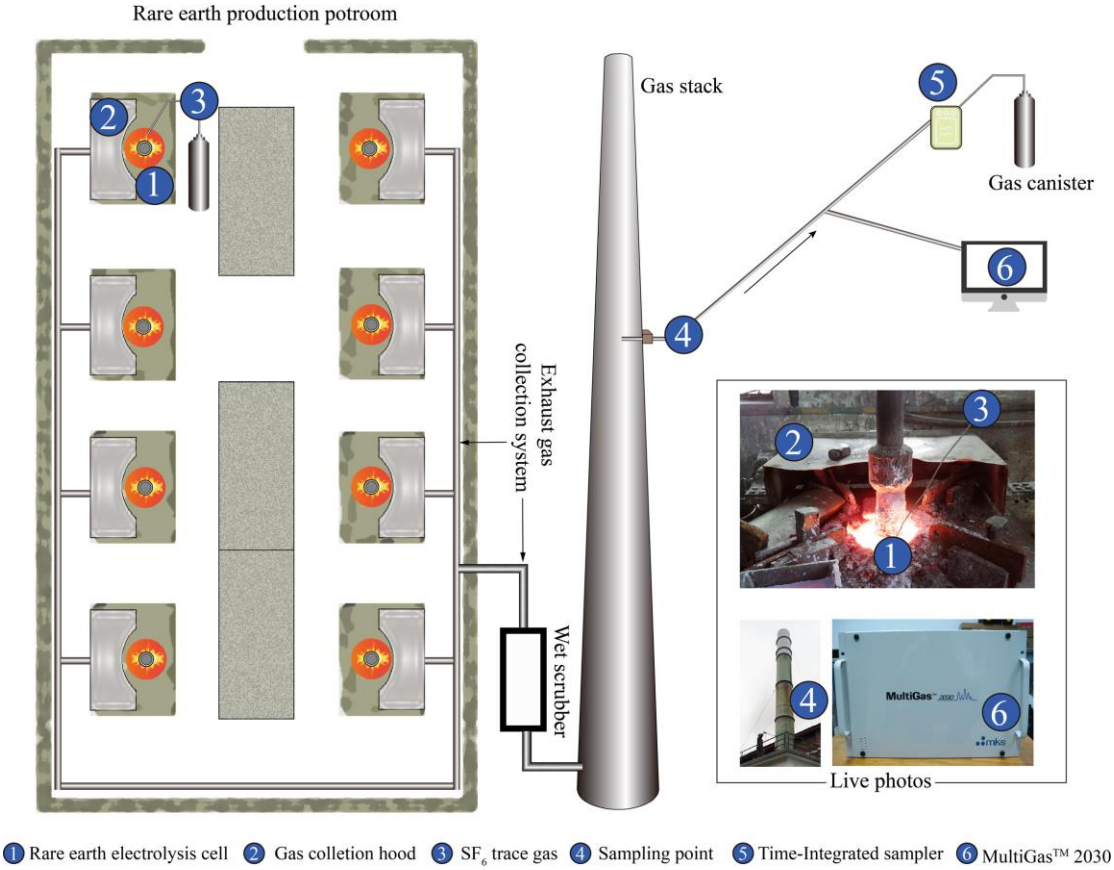

Figure 1: The arrangement for on-site monitoring and sampling of PFCs from a potroom of rare earth electrolysis cells.

2.2. Time-Integrated Sampling and Lab Analysis

Exhaust air was drawn from the exhaust gas stack by pump (M121-FP-BA1-L) through a sampling tube (1/4" OD Synflex tubing, Eaton, USA) at flow rate of 5 L/min to feed both the

in-situ FTIR system and time-integrated sampler. The sampler pressurized into pre-vacuumed 3-L stainless steel canisters (X23-2N, LabCommerce, Inc, USA) by means of a membrane pump (KNF-022, KNF Neuberger, Germany). The integrated flow was constrained by a mass flow controller (GFC17, AALBORG, USA) at a constant flow rate for each integrated sample. The flow rate ranged from 2.5 mL/min to 3.5 mL/min depending on the required integrated time of different samples.

Canister samples were transported to Beijing and analysed with a custom-built '*Medusa*' gas chromatographic system with mass spectrometric detection (Agilent 6890/5975B, USA) for fluorinated greenhouse gases within one month. The system uses the technique developed by the *Advanced Global Atmospheric Gases Experiment* (AGAGE) and was operated in the lab of the *Meteorological Observation Centre* of the *China Meteorological Administration* (MOC/CMA). The measurements are linked to AGAGE standard scales (Prinn et al., 2018) and the precisions are <0.5% for CF_4, C_2F_6, C_3F_8, c-C_4F_8 and C_4F_{10}. The detailed analysis method was described by Zhang et al. (2018). For the samples with pressure less than 10 psi, a dilution procedure was used to pressurize the sample by zero gas to ensure there is enough volume.

2.3. Methodology for Estimating Gas Collection Efficiency using SF_6 Tracer

As illustrated in Figure 1, high concentration SF_6 (0.498%, Beijing Beifenhaipu Gas Industrial, China) was released at a constant flow rate by a mass flow controller (20 to 1000 mL/min depending on the releasing time period) at a chosen cell at each RE potroom. The end of the gas release tubing was placed as close to the anode as possible (generally less than 1 cm away from anodes). Actual gas release periods (i.e. monitoring period) and flow rates at each potroom are listed in Table 2.

SF_6 was diluted in the exhaust gas collection system and later collected into stainless steel canisters together with other greenhouse gases in the exhaust gas. The SF_6 concentration was analyzed by the Medusa-GC/MS in MOC/CMA lab (described in section 2.2) with an uncertainty of 0.5%. Thus, the gas collection efficiency was calculated as follows:

$$E_{col} = \frac{C_{canister} \times F_{exhaust}}{C_{standard} \times F_{standard}} \qquad \text{(Eq. 10);}$$

Here E_{col} is gas exhaust collection efficiency, $C_{canister}$ and $C_{standard}$ are SF_6 concentrations of canister samples and of the SF_6 tracer standard, respectively, while $F_{exhaust}$ and $F_{standard}$ are the flow rates of the exhaust gas and the released flow rate of SF_6 tracer gas (high concentration standard), respectively. Here $C_{standard}$ is 0.489%.

2.4. Estimating Emission Factors of C_2F_6 and C_3F_8

The *MKS MG2030* FTIR is capable of measuring the emission of CF_4 from production lines, yet it is unable to detect the gas emissions such as C_2F_6 and C_3F_8 directly, due to limitations of the reference spectrum used in the FTIR. To estimate emission factors for these two gases, we calculate their emission volumes by referring to the emission volume ratios (which is measured in

the lab from time-integrated samples) between them and CF_4.

The emission factors (*EF*) of C_2F_6 and C_3F_8 can be calculated by the expressions as below:

$$EF_{C2F6} = EF_{CF4} \times (138 / 88) \times (D_{C2F6} / D_{CF4}) \quad \text{(Eq. 11)}$$

$$EF_{C3F8} = EF_{CF4} \times (188 / 88) \times (D_{C3F8} / D_{CF4}) \quad \text{(Eq. 12)}$$

Where, D_{CF4}, D_{C2F6} and D_{C3F8} *are* the average concentration of CF_4, C_2F_6 and C_3F_8 measured in the lab from time-integrated sampling canisters are respectively, and EF_{CF4} is the estimated emission factor of CF_4 (measured simultaneously by FTIR on the same potline).

3. Results and Discussion

3.1. Estimated CF_4 Emission Factors from On-Site FTIR Monitoring

The first FTIR time series data of CF_4 emissions covered 15 pots from the Pr-Nd production potline in Qiandong, over 60 hours of monitoring. As shown in Figure 2, a number of anode effect events, represented by the sharp peaks in CF_4 emissions, were identified. The maximum observed CF_4 concentration was 0.610 ppm. It was estimated that 75% of CF_4 emissions were related to peak or anode effect (AE) emissions, with 25% attributed to 'non-anode effect' (NAE) emissions, as determined by integrating the emission time series for peak vs. non-peak emission periods. Based upon this data, a CF_4 emission factor of 26.66 g/t-RE was calculated, with a corresponding CO_2 equivalent emission factor of 176.76 kg CO_2-e/t-RE. This is roughly 40% lower than the 307.65 kg CO_2-e/t-RE emission factor measured in 2014 for Nd production (Zhang et al., 2018, with emission values converted assuming the same 57.97% gas collection efficiency). This reduction in PFC emissions coincides with the installation of an automated feeding system for the rare earth oxides into the production line over the past 3 years. Therefore, this indicates that improvements to the electrolytic process and operations can reduce PFC emissions.

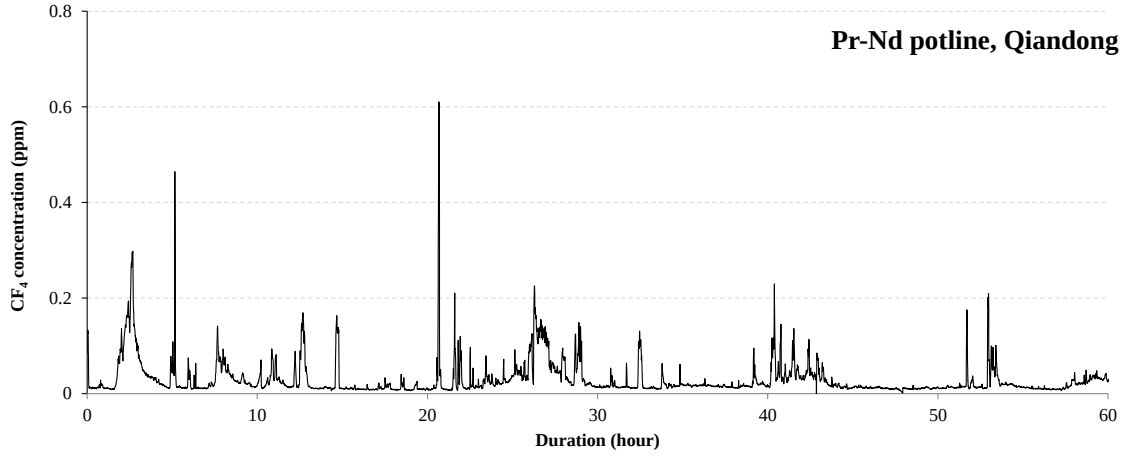

Figure 2: CF_4 concentration of Pr-Nd potline (15 cells) in Qiandong during regular production

There was only one single pot measured in the Dy-Fe potline in Qiandong. To estimate an

emission factor for Dy-Fe production, exhaust gases from the cell was monitored over 24 hours (Figure 3). A series of anode effects (emission peaks) were observed with 3.029 ppm as the maximum concentration of CF_4. Many peak values relating to anode effects were greater than 0.5 ppm; an estimated 91% of CF_4 emissions were related to these AEs, with 9% related to NAE emissions. The overall CF_4 emission factor for Dy-Fe was 109.43 g/t-RE, being equal to 725.52 kg CO_2-e/t-RE. In 2014, the CO_2-equivalent emission factor in this same potline was 1,212.32 kg CO_2-e/t-RE (Zhang et al. 2018, values converted with a 57.97% gas collection efficiency). We can see that the PFC emission had decreased significantly (~40%), which again resulted from improvements to the electrolytic process and material feeding system.

Compared with the other three potlines, the CF_4 emission factor for Dy-Fe production is the highest. One possible explanation is that the voltage for Dy-Fe electrolysis (at 12 V) is much higher than in other potlines (e.g. 4V higher than for the Pr-Nd potline). Operating at higher voltage makes it more likely to trigger anode effects which will produce more PFC gases. Another observation that supports higher PFC emissions is the fact that significantly more fluoride electrolyte is consumed in this Dy-Fe potline, with a two-fold greater fluoride consumption than Pr-Nd production. This is because more anode effects happened in this potline (Figure 3) which led to more PFC emissions. Finally, it should be stressed that there is a level of uncertainty in these results given that Dy-Fe sampling was conducted from only one cell, instead of multiple cells as discussed previously.

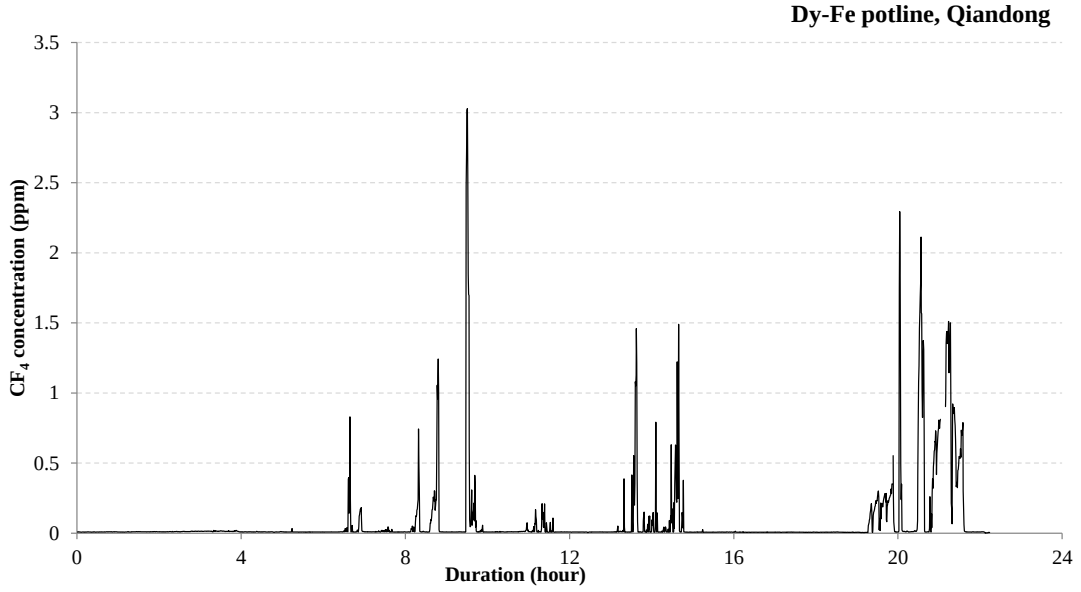

Figure 3: CF_4 concentration of Dy-Fe potline (1 cell) in Qiandong during regular production

The La potline in Qiandong included 6 pots and monitoring was conducted over 36 hours (Figure 4). Similar to the other observations, a number of anode effect events were also captured and the maximum concentration of CF_4 was 0.194 ppm. An estimated 61% of emissions were attributed to AEs, with 39% attributed to NAE emissions. The overall CF_4 emission factor was 36.16 g/t-RE and the CO_2-equivalent emission factor was 239.74 kg CO_2-e/t-RE.

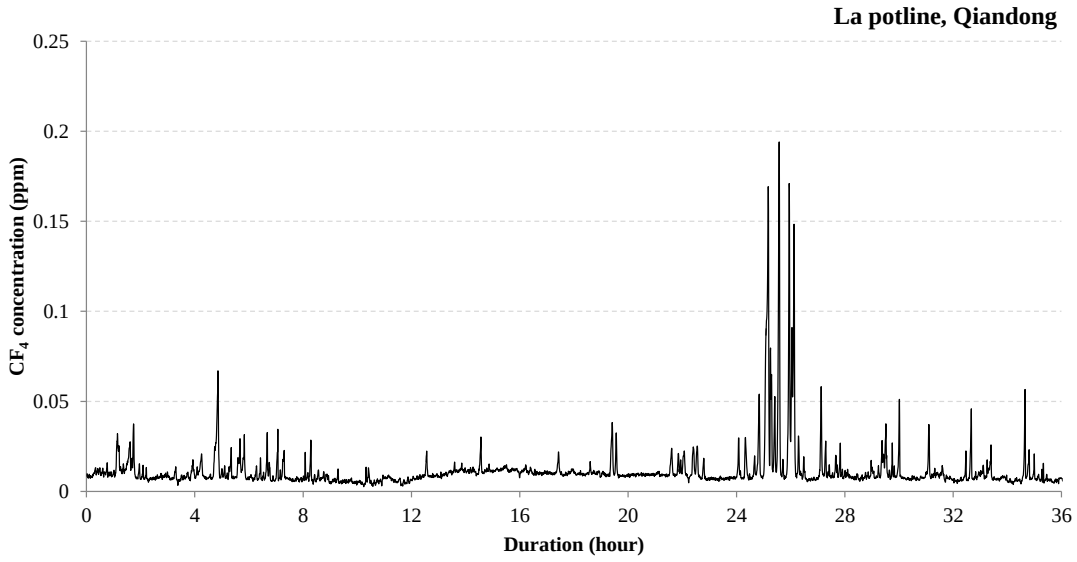

Figure 4: CF_4 concentration of La potline (6 cells) in Qiandong during regular production

At the Ionic Rare Earth Centre, the Pr-Nd potline which had 6 pots was monitored over 36 hours (Figure 5). Anode effect events were not so frequent compared to other potlines, as shown by fewer peak emission events. However, when they did occur, peak emissions were greater than that in the other Pr-Nd potline at Qiandong, with a maximum CF_4 concentration of 0.728 ppm. In terms of total CF_4, an estimated 53% were attributed to AEs, 47% to NAE emissions. A CF_4 emission factor of 33.96 g/t-RE was determined for this potline, equal to 225.15 kg CO_2-e/t-RE.

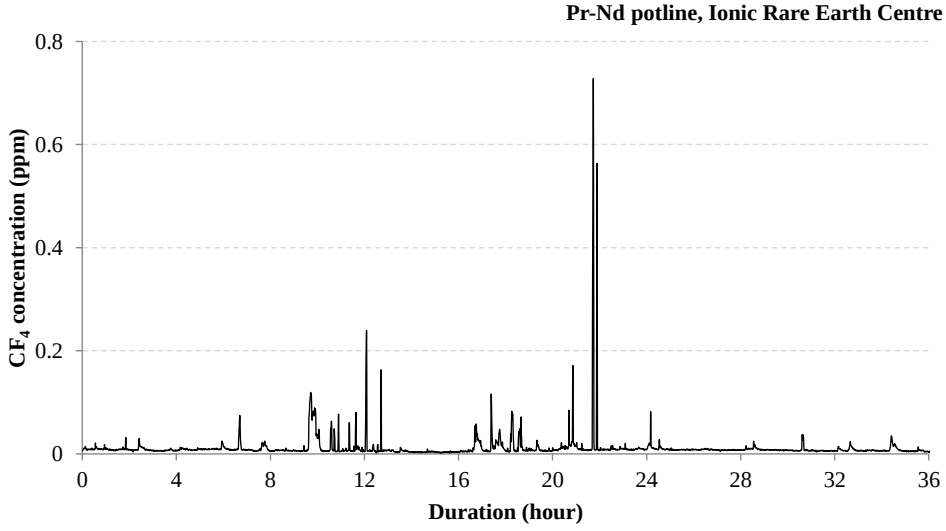

Figure 5: CF_4 concentration of Pr-Nd potline (8 pots) in Ionic Rare Earth Centre during regular production

Originally, plans were made to examine the effect of line current and different cell technologies on PFC emissions, by measuring PFC emissions from Pr-Nd potlines at three companies for >=24 hours, each with varying line current (Table 1). However at Jiangxi South, continuous monitoring was interrupted after only 8 hours when the company had to change the settings of the potline and the production equipment. Furthermore, no AE events were observed

during the 8 hours of monitoring and therefore emission factors based on this data would likely be an under-estimate of actual emission intensities. Therefore, monitoring data and a corresponding emission factor for Jiangxi South's Pr-Nd potline have not been included here. Unfortunately, this meant that emission factors for a higher-amperage cell technology (>10 kA) could not be estimated.

Table 2 summarizes the emission factors CF_4 for all four potlines (excluding Jiangxi South), alongside relevant technical process data, determined gas collection efficiencies and parameters relating to the gas sampling. As explained previously, for the same rare earth metal the magnitude of PFC emissions can vary considerably with the operating line current. Therefore, it is crucial to clearly highlight the current while calculating the emission factor. Moreover, it is crucial to take into account the gas collection efficiency at each company when determining emission factors to ensure fugitive gas emissions that escape the exhaust gas collection system are accounted for.

From SF_6 tracer studies, the gas collection efficiency at both Qiandong and Ionic Rare Earth Center was found to be approximately 57%. At Jiangxi South, this was around 53%, being slightly lower. Therefore, significant improvement in gas collection efficiency cannot be achieved by only small changes to potroom conditions with no fundamental innovation of the current electrolysis technology.

From Table 2, it is clear that estimated CF_4 emission factors vary significantly from one RE metal/alloy to another. For production of Pr-Nd alloy, CF_4 emission factors also varied between different companies, with CF_4 emissions at Ionic Rare Earth Center being roughly 80% that at Qiandong. It is possible that this is due to fluctuation of gas collection efficiency over time at each company, due to smelter workers' frequent adjustments of the gas collection hoods during monitoring (each company had differing gas collection systems). Furthermore, this might also be attributed to differences in process operating conditions (temperature, voltage, etc, as might be suggested by differences in net anode carbon consumption in Table 2).

Also summarized in Table 2 are the contribution of AEs (peak emission events) to total CF_4, ranging from 53% to 91% over the four potlines with valid data. These highlight that PFCs can also be generated *outside* of an anode effect condition. As a point of discussion, since no anode effects were detected during Jiangxi South monitoring (data not shown here), AE-related emissions could not be estimated and therefore all measured CF_4 was attributed to NAE emissions. Again, the 8 hours of monitoring at this production line was deemed insufficient to provide a meaningful representation of emissions performance at this company and hence emission factors were not calculated.

Table 2: The emission factor of CF_4 for different production lines based on on-site monitoring

Company	Qiandong			Ionic Rare Earth Center
Potline	*Pr-Nd*	*Dy-Fe*	*La*	*Pr-Nd*
Gas flow rate at the sampling point (Nm^3/h)	12,000	1,340	17,066	18,327
Diameter of the gas stack (m)	1.2	0.2	0.8	0.6
Production of RE metal (t/d)	2.173	0.150	0.930	0.965
Net anode carbon consumption (kg-C/t-RE)	136.5	166.6	144.3	160
Gas collection efficiency (%)	57.97	57.97	57.97	56.22
Emission factor of CF_4 (g/t-RE)	26.66	109.43	36.16	33.96
% CF_4 emissions related to AEs	75%	91%	61%	53%

3.2. Estimation of C_2F_6 and C_3F_8 emission factors from Time-Integrated Sampling & Lab Analysis

Analysis of time-integrated canister samples in the laboratory provided significantly higher sensitivities in detecting greenhouse gases. Analysis results confirmed that addition to CF_4, C_2F_6 and C_3F_8, enhanced concentrations (concentration of exhaust gas minus background samples) of two other PFCs were observed in part of the samples, namely c-C_4F_8 and C_4F_{10}. However, it was found that for all four potlines (Jiangxi South excluded), the ratio of the enhanced concentrations of c-C_4F_8 and C_4F_{10} to CF_4 were <0.05%. This ratio was so low that no further emission factor estimation was conducted for these gases.

Concentration ratios of C_2F_6 and C_3F_8 to CF_4 are presented in Table 3. It is clear that, in all potlines regardless of line current and potroom conditions, CF_4 is consistently the dominant PFC gas emitted, taking up more than 90% of total PFCs detected. Furthermore, while C_3F_8 cannot be ignored (compared to c-C_4F_8 and C_4F_{10}), it contributes to less than 1% of total PFCs and is at the lowest concentration amongst the three main PFC gases of interest.

By referring to the obtained CF_4 emission factors from FTIR measurements (Table 2) and the corresponding concentration ratios determined from the lab analysis of time-integrated samples (Table 3), emission factors of C_2F_6 and C_3F_8 from each potline then can be calculated by

Eq. 11 and Eq. 12. Interestingly, the mass ratio of EF_{C2F6} / EF_{CF4} in two Qiandong potlines (Pr-Nd and Dy-Fe) is similar to the 10% ratio typically found in aluminium electrolysis (IAI, 2017), while the other two RE potlines differed as is the case for different technology cells in aluminium (IAI, 2017).

As presented in Table 3, Qiandong *Dy-Fe alloy* and *La* potlines had C_2F_6 emission factors of 10.95 g/t-RE and 0.26 g/t-RE, respectively, and C_3F_8 emission factors of 0.03 g/t-RE and 0.10 g/t-RE, respectively. Foreseeably, the emission factors of both C_2F_6 and C_3F_8 for Pr-Nd alloy production lines in Qiandong differ from that in the Ionic Rare Earth Center. Specifically, in Qiandong the C_3F_8 emission factor is 0.19 g/t-RE, almost 30% lower than that in Ionic Rare Earth Center; this is not surprising, given that CF_4 emission factors were also ~20% lower at Qiandong. Interestingly, for C_2F_6, the outcome from Qiandong is 2.98 g/t-RE, around 70% lower than that from Ionic Rare Earth Center, given the ratio of C_2F_6 to CF_4 at Ionic Rare Earth Centre is almost 3 times higher.

Table 3: The estimated emission factors (EF) for C_2F_6 and C_3F_8

Company		Qiandong			Ionic Rare Earth Center
Potline		*Pr-Nd*	*Dy-Fe*	*La*	*Pr-Nd*
No. of pots		15	1	6	6
Line current (kA)		5	5	5	6
Conc. Ratio	D_{C2F6} / D_{CF4}	0.0714	0.06384	0.0046	0.2033
	D_{C3F8} / D_{CF4}	0.00355	0.00015	0.0013	0.0037
EF Mass Ratio	EF_{C2F6} / EF_{CF4}	0.1119	0.1001	0.0072	0.31882
	EF_{C3F8} / EF_{CF4}	0.0076	0.00031	0.0028	0.0079
EF_{CF4} (g/t-RE)		26.66	109.43	36.16	33.96
EF_{C2F6} (g/t-RE)		2.98	10.95	0.26	10.83
EF_{C3F8} (g/t-RE)		0.19	0.03	0.10	0.27

3.3. Uncertainty Analysis

Due to uncontrollable factors in monitoring, the estimated emission factors inevitably have statistically errors which should not be ignored. From Eq. 9, we can infer that the uncertainty pertaining to CF_4 emission factor mainly comes from three aspects, which are the measurement of the emission concentration, of the gas flow rate and of the gas collection efficiency. Suppose the relative standard deviations in these three aspects are ε_{CF4}, ε_F, ε_{Ecol}, the relative standard error (ε_R)

is calculated as below:

$$\varepsilon_R = \left(\varepsilon_{CF4}^2 + \varepsilon_F^2 + \varepsilon_{Ecol}^2\right)^{1/2} \qquad \text{(Eq. 13)}$$

$$U_{CF4} = EF_{CF4} \times \varepsilon_R \qquad \text{(Eq. 14)}$$

and the results are listed in Table 4.

It is necessary to keep information in these aspects as reference for further estimation of global CO_2 equivalent emission from rare earth metal electrolysis.

Table 4: CO_2 equivalent emission factors and uncertainty of PFC emissions

Company		QianDong			Ionic Rare Earth Center
Pot line		*Pr-Nd*	*Dy-Fe*	*La*	*Pr-Nd*
EF_{CF4}	g-CF_4/t-RE	26.66±2.24	109.43 ±9.63	36.16 ±3.04	33.96 ±1.56
	kg CO_2-e/ t-RE	176.76±14.84	725.52 ±63.85	239.74 ±20.14	225.15 ±10.36
EF_{C2F6}	g-C_2F_6/t-RE	2.98±0.28	10.95±1.08	0.26±0.02	10.83±0.71
	kg CO_2-e/ t-RE	33.11±3.15	121.59±12.04	2.89±0.28	120.18±7.93
EF_{C3F8}	g-C_3F_8/t-RE	0.19±0.02	0.03±0.01	0.10±0.01	0.27±0.02
	kg CO_2-e/ t-RE	1.73±0.16	0.30±0.09	0.90±0.09	2.39±0.16
Total PFC EF (kg CO_2-e/t-RE)		211.60±18.16	847.41±75.97	243.53±20.50	347.72±18.45

3.4. Discussion on PFC Emission Factors

Using GWPs for the three main PFCs of interest – CF_4, C_2F_6 and C_3F_8 – a converted CO_2-equivalent emission factor for total PFCs can be estimated for the four potlines (Table 4). All emission factors except that for *Dy-Fe* alloy production are lower than 350 kg CO_2-e/t-RE, an equivalent target level for the Chinese aluminium industry by 2020. This highlights the importance of focusing on reducing PFC emissions from *Dy-Fe* alloy production, which had the highest emissions intensity from this study and the 2014 study (Zhang et al., 2018).

It is also pertinent to compare the rare earth PFC emission factors determined in this work with those from the aluminium industry. When compared to Chinese aluminium industry's 2020 target of 350 kg CO_2-e/t-Al and the global aluminium industry's 2016 overall PFC emission intensity of 640 kg CO_2-e/t-Al (estimated global emission factor from the 2016 IAI Anode Effect Survey (2017), albeit using GWPs from the IPCC Fourth Assessment Report), this implies that in most situations PFC emissions intensity (on a mass basis) from rare earth metal electrolysis is on a lower or similar order of magnitude to emissions from aluminium electrolysis. Note that for fundamental understanding of PFC generation, the molar mass of rare earth metals (e.g. Nd at 144 g/mol) is roughly 5 times greater than that of aluminium (27 g/mol); therefore, PFC emission

intensities for rare earth metals are 5 times greater on a mole-basis than for aluminium. For the practical purpose of emissions accounting from industry however, it is more appropriate to compare emission intensities by mass.

In a general sense, the rare earth metal production settings such as cell size, voltage and current have an evident impact upon the PFC emissions. For instance, high cell voltage operation (e.g. on Dy-Fe cells) can result in more fluoride participating in the electrolysis reaction, thus generating more anode effects which results in more frequent spikes in PFC emission. Therefore, emission factors determined for each of the four potlines should be attached with information that describes these settings.

Moreover, it is worth emphasising again that the high emission factor for Dy-Fe alloy has been based upon observed data from only one single pot. Inevitably it incurs the risk of uncertainty and may be less representative for *Dy-Fe* alloy production. Nonetheless, we retained this data so as to maintain coverage over production multiple rare earth metals. In any case, this salient value presents us with a necessity to explore the underlying causes that lead to greater emissions and formulate effective solutions to reduce them in *Dy-Fe* alloy production.

The comparison of AE-related emissions (ranging from 53% to 91%) vs. NAE-related emissions is also of particular interest since (1) it highlights that PFC emissions can be generated on industrial cells outside of an anode effect and (2) similar NAE-emissions have also been found in industrial aluminium electrolysis (Wong et al., 2015) and are now known in that industry to be difficult to detect, both by operators and control systems. In contrast, AE-related emissions are often correlated with high-voltage events on cells, which can be used to detect, mitigate and account for AE-related emissions. Applied to the rare earths industry, this would mean NAE-related PFC emissions will be difficult to detect and account for (without sophisticated instrumentation) and more importantly to mitigate.

Finally, the current study provides much greater coverage than previous studies in providing PFC emission factors for multiple gases (CF_4, C_2F_6, C_3F_8) from three of the most common rare earth metals produced by electrolysis. However, given the lack of valid data from Jiangxi South, no conclusive observations can be made as to the impact of line-current on emissions intensity. This would be a good area of focus for further studies by the industry into PFCs from rare earths.

4. Conclusions

Through on-site FTIR monitoring and lab analysis of time-integrated samples, it was confirmed that in addition to CF_4 there are four other PFC emissions in the exhaust gas from industrial rare earth electrolysis, namely: C_2F_6, C_3F_8, c-C_4F_8 and C_4F_{10}. While these four components could not be measured directly by the FTIR, time-integrated samples obtained during on-site monitoring were analysed in the lab using a custom-built ‘Medusa’ GC-MS system. The result shows that in all the four examined potlines (Pr-Nd, Dy-Fe and La production at Qiandong and Pr-Nd production at the Ionic Rare Earth Center), CF_4 is absolutely the primary PFC component, accounting for roughly 90% of PFC gases by mass. The concentration ratio of both C_2F_6 and C_3F_8 to CF_4 differs somewhat across these four pot lines – for C_2F_6 it is roughly 10% wt (similar to that in industrial aluminium electrolysis) and for C_3F_8 the ratio is less than 1% wt. As the ratios of the enhanced concentrations of c-C_4F_8 and C_4F_{10} to CF_4 across four potlines are both

less than 0.05%, calculation of their emission factors was not conducted in this research.

Emissions vary from one rare earth metal to another and from company to another for the same metal. In general, PFC emission intensities for most rare earth metals are of a lower level of magnitude (by-mass) compared to industrial aluminium electrolysis, with the exception of Dy-Fe electrolysis. Factors behind the variation in emissions intensity include not only electrical line current, but also cell design, operating conditions and process technology employed – as shown by reductions in Pr-Nd emissions intensity at Qiandong smelter after improvements to oxide feeding technology (Zhang et al, 2018 vs. this work) – and as highlighted by differences in operating voltage, fluoride consumption and anode carbon consumption. Unfortunately, comparison of emission intensities across low vs. high-amperage cell technologies was inconclusive, given the lack of valid data at Jiangxi South smelter.

5. Acknowledgements

The authors of this work acknowledge all parties involved in the measurement team and the three rare earth companies that participated in the research: *Qiandong Rare Earths Group Co. Ltd*, *National Engineering Research Center for Ionic Rare Earth* and *Jiangxi South Rare Earth High Tech. Co. Ltd*. We would also like to give our special thanks for the funding support from the following institutions: (1) An Emission-Transport-Exposure Model Based Study on the Evaluation of the Environmental Impact of Carbon Market (Grant No. 71673107) and a fluorinated greenhouse emission study (Grant No. 41575114), both supported by the National Natural Science Foundation of China; (2) The Recruitment Program of Global Experts (Youth Group) of China (Grant No. D1218006); and (3) Technology Innovation Foundation of Hubei Province (Grant No. 2017ADC073).

6. References

Chase R, Gibson R and Marks J. (2005) PFC emissions performance for the global primary aluminum industry. In: Kvande H (ed) *Light Metals.* 279-282.

Fraser P., Steele P., Cooksey M. (2013) PFC and Carbon Dioxide Emissions from an Australian Aluminium Smelter Using Time-Integrated Stack Sampling and GC-MS, GC-FID Analysis. In: Sadler B.A. (eds) Light Metals 2013. The Minerals, Metals & Materials Series. Springer, Cham. https://doi.org/10.1007/978-3-319-65136-1_148

International Aluminium Institute (IAI), World Aluminium–Alumina Production (2014), Available from: http://www.world-aluminium.org/statistics/alumina-production/.

International Aluminium Institute (IAI), Results of the 2016 Anode Effect Survey: Report on the Aluminium Industry's Global Perfluorocarbon Gases Emissions, Available from: http://www.world-aluminium.org/media/filer_public/2017/07/26/2016_anode_effect_survey_result_2017.pdf

IPCC. (2006) 2006 Ipcc Guidelines for National Greenhouse Gas Inventories. Japan: IGES, 2006.

IPCC. (2006) 2006 IPCC Guidelines for National Greenhouse Gas Inventories: Japan: IGES, 2006.List of Contributing Authors, Available from: https://www.ipcc-nggip.iges.or.jp/public/2006gl/pdf/0_Overview/V0_3_Contributor.pdf

IPCC. (2013) Climate Change 2013: The Physical Science Basis. Contribution of Working Group I to the Fifth Assessment Report of the Intergovernmental Panel on Climate Change. Cambridge, United Kingdom and New York,USA: Cambridge University Press.

Kim, J., et al. (2014), Quantifying aluminum and semiconductor industry perfluorocarbon emissions from atmospheric measurements, *Geophys. Res. Lett.*, *41*, 4787–4794, doi:10.1002/ 2014GL059783.

Kjos, O.S., Solheim, A., Aarhaug, T. Osen, K.S., Martinez, A.M., Sommerseth, C., Gudbrandsen H., Støre, A. & Gaertner, H. (2018) PFC evolution characteristics during aluminium and rare earth electrolysis, In: *TMS Light Metals*, paper to be presented at Phoenix, Arizona, March 11-15, 2018.

Liu W. (2008) The development of China sintered ND-Fe-B magnets industry and its manufacture techniques. *Metal World* 15(6): 38-41.

Myhre, G., D. Shindell, F.-M. Bréon, W. Collins, J. Fuglestvedt, J. Huang, D. Koch, J.-F. Lamarque, D. Lee, B. Mendoza, T. Nakajima, A. Robock, G. Stephens, T. Takemura and H. Zhang, 2013: Anthropogenic and Natural Radiative Forc- ing. In: *Climate Change 2013: The Physical Science Basis. Contribution of Working Group I to the Fifth Assessment Report of the Intergovernmental Panel on Climate Change* [Stocker, T.F., D. Qin, G.-K. Plattner, M. Tignor, S.K. Allen, J. Boschung, A. Nauels, Y. Xia, V. Bex and P.M. Midgley (eds.)]. Cambridge University Press, Cambridge, United Kingdom and New York, NY, USA. Available from: https://www.ipcc.ch/pdf/assessment-report/ar5/wg1/WG1AR5_Chapter08_FINAL.pdf

Prinn, R. G., Weiss, R. F., Arduini, J., Arnold, T., DeWitt, H. L., Fraser, P. J., Ganesan, A. L., Gasore, J., Harth, C. M., Hermansen, O., Kim, J., Krummel, P. B., Li, S., Loh, Z. M., Lunder, C. R., Maione, M., Manning, A. J., Miller, B. R., Mitrevski, B., Mühle, J., O'Doherty, S., Park, S., Reimann, S., Rigby, M., Saito, T., Salameh, P. K., Schmidt, R., Simmonds, P. G., Steele, L. P., Vollmer, M. K., Wang, R. H., Yao, B., Yokouchi, Y., Young, D., and Zhou, L.:(2018) History of Chemically and Radiatively Important Atmospheric Gases from the Advanced Global Atmospheric Gases Experiment (AGAGE), *Earth Syst. Sci. Data Discuss.*, https://doi.org/10.5194/essd-2017-134, in review

Ren LK, She CJ and Wei XJ. (2001) Analysis of anodic gases in neodymium electrolysis. *Chinese Journal of Nonferrous Metals*.

Rhoderick G, Chu P, Dolin E, et al. (2001) Development of perfluorocarbon (PFC) primary standards for monitoring of emissions from aluminum production. *Fresenius Journal of Analytical Chemistry* 370(7): 828-833.

Tabereaux AT. (1994) Anode effects, PFCs, global warming, and the aluminum industry. *JOM* 46(11): 30-34.

U.S. Geological Survey, Mineral Commodity Summaries—Rare Earths (Reston, VA: U.S. Geological Survey, 2014), pp. 128–129.

Vogel, H., Flerus, B., Stoffner, F. & Friedrich, B. (2017a) Reducing Greenhouse Gas Emission from the Neodymium Oxide Electrolysis. Part I: Analysis of the Anodic Gas Formation. *Journal of Sustainable Metallurgy* **3**(1): 99-107.

Vogel, H. & Friedrich, B. (2015) Development and Research Trends of the Neodymium Electrolysis – A Literature Review. In: *8th European Metallurgical Conference (EMC)*, Dusseldorf, Germany.

Vogel H and Friedrich B. (2017b) Reducing Greenhouse Gas Emission from the Neodymium Oxide Electrolysis. Part II: Basics of a Process Control Avoiding PFC Emission. *International Journal of Nonferrous Metallurgy* 06(3): 27-46.

Wen H, Kuang G and Mao J. (2012) 25 KA rare earth electrolytic cell for fluoride molten salt system Beijing: China's State Intellectual Property Office, 1-6.

Wong DS, Fraser P, Lavoie P, et al. (2015) PFC Emissions from Detected Versus Nondetected Anode Effects in the Aluminum Industry. *JOM* 67(2): 342-353.

Wen, H., Kuang, G. & Mao, J. (2012) 25 KA rare earth electrolytic cell for fluoride molten salt system. In: ed. China's State Intellectual Property Office, pp. 1-6. China.

Gen Zhang , Bo Yao, Martin K. Vollmer, Stephen A. Montzka, Jens Mühle, Ray F. Weiss, Simon O'Doherty, Yi Li, Shuangxi Fang, Stefan Reimann (2017). Ambient mixing ratios of atmospheric halogenated compounds at five background stations in China. Atmospheric Environment 160: 55-69. http://dx.doi.org/10.1016/j.atmosenv.2017.04.017.

Zhang, L., Wang, X., & Gong, B. (2018). Perfluorocarbon emissions from electrolytic reduction of rare earth metals in fluoride/oxide system. *Atmospheric Pollution Research*., 9(1): 61-65.

Zhao CF, Zhang SC, Huang X, et al. (2008) Study of PFC emission in aluminum industry. *Light Metals*